Macromolecules

Article

pubs.acs.org/Macromolecules

Predicting the Mechanical Properties of Organic Semiconductors Using Coarse-Grained Molecular Dynamics Simulations

Samuel E. Root, Suchol Savagatrup, Christopher J. Pais, Gaurav Arya,* and Darren J. Lipomi*

Department of NanoEngineering, University of California San Diego, 9500 Gilman Drive, Mail Code 0448, La Jolla, California 92093-0448, United States

Supporting Information

ABSTRACT: The ability to predict the mechanical properties of organic semiconductors is of critical importance for roll-to-roll production and thermomechanical reliability of organic electronic devices. Here, we describe the use of coarse-grained molecular dynamics simulations to predict the density, tensile modulus, Poisson ratio, and glass transition temperature for poly(3-hexylthiophene) (P3HT) and its blend with C_{60}. In particular, we show that the resolution of the coarse-grained model has a strong effect on the predicted properties. We find that a one-site model, in which each 3-hexylthiophene unit is represented by one coarse-grained bead, predicts significantly inaccurate values of density and tensile modulus. In contrast, a three-site model, with one coarse-grained bead for the thiophene ring and two for the hexyl chain, predicts values that are very close to experimental measurements (density = 0.955 g cm^{-3}, tensile modulus = 1.23 GPa, Poisson ratio = 0.35, and glass transition temperature = 290 K). The model also correctly predicts the strain-induced alignment of chains as well as the vitrification of P3HT by C_{60} and the corresponding increase in the tensile modulus (tensile modulus = 1.92 GPa, glass transition temperature = 310 K). We also observe a decrease in the radius of gyration and the density of entanglements of the P3HT chains with the addition C_{60} which may contribute to the experimentally noted brittleness of the composite material. Although extension of the model to poly(3-alkylthiophenes) (P3ATs) containing side chains longer than hexyl groups—nonyl (N) and dodecyl (DD) groups—correctly predicts the trend of decreasing modulus with increasing length of the side chain measured experimentally, obtaining absolute agreement for P3NT and P3DDT could not be accomplished by a straightforward extension of the three-site coarse-grained model, indicating limited transferability of such models. Nevertheless, the accurate values obtained for P3HT and P3HT:C_{60} blends suggest that coarse graining is a valuable approach for predicting the thermomechanical properties of organic semiconductors of similar or more complex architectures.

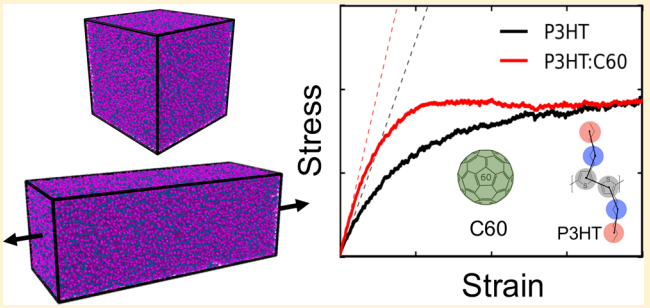

INTRODUCTION

One key feature of organic semiconductors that distinguishes them from their inorganic counterparts is the potential to manufacture lightweight devices such as organic solar cells and field-effect transistors that exhibit extreme mechanical compliance and durability.[1,2] Recent advances in synthetic organic chemistry along with careful tuning of materials processing have produced many organic semiconductors with broad optical absorptions and large charge-carrier mobilities.[3] Various design rules and computational methods have been developed for studying and predicting the optoelectronic properties of candidate materials;[4−6] however, much less effort has been dedicated to understanding the thermomechanical behavior of these materials.[7] In fact, thermomechanical properties like glass transition temperature, tensile modulus, and toughness are of critical importance for stretchable, ultraflexible, portable, and wearable applications. Moreover, these properties depend strongly on molecular structure (e.g., the backbone architecture and the length and branching of the alkyl side chain) and are difficult to predict based on intuition alone. An improved understanding of these structure−property relationships will greatly aid in the design of reversibly stretchable semiconducting polymers for applications requiring mechanical robustness and stability. This paper describes the first use of coarse-grained molecular dynamics simulations for the determination of the thermal and mechanical properties of a conjugated polymer and its blend with C_{60}.

Molecular dynamics (MD) simulations offer an attractive means for elucidating the mechanical properties of polymeric systems, and various atomistic models have already been applied to and validated for commodity polymers and engineering plastics, such as polyolefins.[8−11] Because of the vast difference in the characteristic time scales of the fastest dynamic mode (covalent bond vibrations) and the slowest mode (chain reptation) of typical polymers, coarse-grained (CG) models are often required for computationally efficient simulations.[12−15] These models treat chemically bonded groups of atoms as single CG beads that interact with other CG beads,

Received: January 28, 2016
Revised: March 15, 2016
Published: March 31, 2016

DOI: 10.1021/acs.macromol.6b00204
Macromolecules 2016, 49, 2886−2894

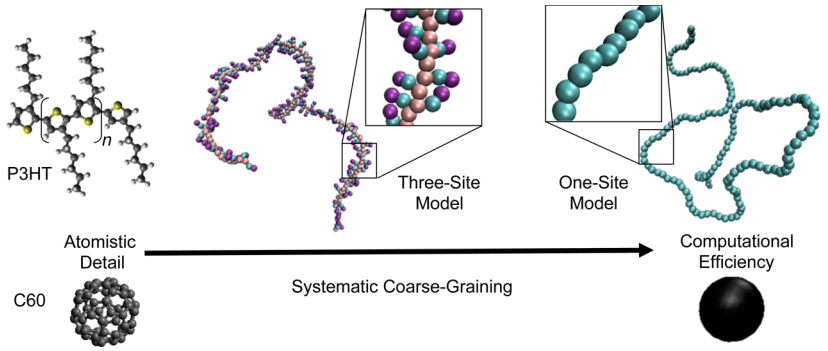

Figure 1. Diagram showing the chemical structures of P3HT polymer and C_{60} fullerene along with the various levels of CG models investigated in this study.

within and across chains, using effective CG potentials that are chosen to reproduce as closely as possible the structural and thermodynamic properties of the polymers obtained from atomistic simulations or experiments. From the point of view of MD simulations, such coarse-graining leads to enormous reductions in the number of simulated particles and considerable softening of interparticle interactions, allowing for the simulation of *larger* systems with *longer* time steps than is possible with fully atomistic models. One widely used method for deriving such CG models is the so-called iterative Boltzmann inversion (IBI) approach.[16] In this approach, probability distributions describing specific inter- and intramolecular degrees of freedom obtained from atomistic simulations are used to iteratively adjust the effective potentials of the CG model until it yields similar distributions as those obtained from the atomistic models.

In this study, we investigated the use of CG molecular dynamics to understand and predict the mechanical properties of a model conjugated polymer: poly(3-hexylthiophene) (P3HT). First we determined the effect of the resolution of the CG model, shown in Figure 1, on the predicted mechanical properties. Through comparison to experimentally obtained values of the tensile modulus, glass transition temperature, and density, we determined the optimal CG resolution to achieve computationally viable simulations while retaining only the most essential chemical details that govern the macroscopic mechanical behavior of these systems. Next, we showed that in agreement with experiment, the addition of a fullerene electron acceptor (to form a bulk heterojunction, the active layer of an organic solar cell) increased both the glass transition while simultaneously reducing the entanglement density and radius of gyration of the P3HT chains. Finally, we investigated the effect of alkyl side-chain length on the thermomechanical properties of poly(3-alkylthiophenes) (P3ATs) to show that the increase in the side chain length produces a material with greater compliance. On the basis of our results, we identified the advantages and limitations of using CG modeling to predict the thermomechanical properties of this important class of materials.

COMPUTATIONAL DESIGN

Model System. We chose P3HT as the model system for this study because it is one of the most well understood semiconducting polymers in the literature.[17] The availability of various atomistic and CG models along with extensive experimental characterization makes P3HT an ideal subject for evaluating the predictive capabilities of the proposed computational methodology. Several studies have performed quantum mechanical calculations to parametrize atomistic models of P3HT.[18−20] In particular, DuBay et al. have shown that applying generic force fields (optimized for simple organic liquids) result in significant inaccuracies with respect to dihedral distributions and persistence length and that parameters to describe these interactions must in general be obtained from *ab initio* calculations.[19] In recent studies, Tummala et al. have used an accurate atomistic model to study the effect of molecular weight and entanglement on the elastic properties of P3HT as well as blends with fullerenes.[21,22] The authors demonstrated good agreement between simulation and experiment, finding that oligomers containing at least 50 monomers were required to observe elastic behavior, and evaluated the effect of the fullerene acceptor side-chain chemistry on the mechanical properties.

In the past few years, several CG models for P3HT have been developed,[23−29] but these models have not been applied to predict thermomechanical properties. In this work, we evaluated the viability of two of these models, as depicted in Figure 1, to make such predictions. These models were chosen because they were both systematically parametrized from atomistic simulations using the IBI procedure.[16] We chose to compare the one-site model developed by Lee et al.[26] with the three-site model developed by Huang et al.[23,30] to examine the effect of the resolution of the model on the predicted thermomechanical properties. In the one-site model, the entire 3-hexylthiophene monomer (25 atoms) is mapped onto a single CG bead, while for the three-site model, the thiophene ring is mapped onto a single CG bead and the hexyl side chain is represented by two CG beads.

Computational Methods. The starting configuration for each system was generated by growing 300 polymer chains with 150 monomers each at a low density (0.01 g cm^{-3}) within a periodic simulation box by using equilibrium bond length and angle values and sampling the intermonomer dihedral angles from a Boltzmann distribution. This chain length was chosen to best match the average molecular weight (~25 kDa) of our experimental values available for comparison. We used 300 chains to ensure that the length of the simulation box was greater than twice the average radius of gyration of the polymer chains to eliminate system size effects such as polymer chains entangling with their own periodic images.[31] We note that to simulate a system of this size using atomistic simulations would require explicit consideration of more than 1 million atoms whereas the CG simulations require only 135 000 CG beads

DOI: 10.1021/acs.macromol.6b00204
Macromolecules 2016, 49, 2886−2894

and 45 000 CG beads for the three-site model and the one-site model, respectively.

To model the solid polymer structure obtained in a standard coating procedure (e.g., spin-coating) from a good solvent (e.g., *o*-dichlorobenzene) without explicitly considering solvent molecules, the interaction energies were decreased to 10% of their condensed phase values. Langevin dynamics were employed to implicitly include the effects of solvent friction and random collisions with solvent molecules;[32] following Schwarz et al.,[24] a friction factor of $\gamma = (180\ \text{fs})^{-1}$ was used to simulate a viscous solvent. Gradually over the course of ∼100 ns, the interaction strengths were restored to their condensed phase values, and the system box dimensions were allowed to relax until the density converged and fluctuated about its equilibrium value in the melt state. This process was simulated at 550 K using a Nosé−Hoover style barostat set to 1 atm with a damping parameter of 2000 fs. Time steps of 10 and 4 fs were used for the one-site and three-site model, respectively; we note that the lower-resolution model allows for the use of a larger time step. An illustration of this procedure applied to a P3HT:C_{60} (1:1 mass fraction) bulk heterojunction is shown in Figure 2a.

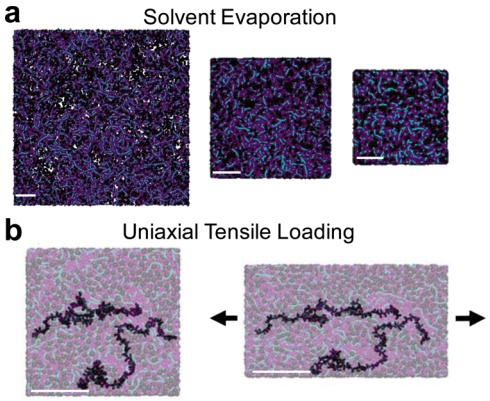

Figure 2. Schematic renderings of simulation process applied to a P3HT:C_{60} bulk heterojunction. (a) The formation of a solid film by evaporation with implicit solvent molecules. (b) Uniaxial tensile loading with two representative chains highlighted in black; the arrows indicate the direction of applied strain. The scale bar is 10 nm.

In the next step, the system was cooled gradually from 550 to 100 K in intervals of 20 K using a Nosé−Hoover thermostat with a time constant of 1000 fs; the interval length was chosen so that the density had time to stabilize during each interval. This procedure was used to calculate the density as a function of temperature and provide an estimate for the glass transition temperature, which is taken to be the point at which there is a discontinuity in the thermal expansion coefficient.

Finally, as illustrated in Figure 2b, a uniaxial tensile deformation was applied to the quenched system with amorphous morphology obtained at 300 K; this was achieved by imposing a constant strain rate ($1 \times 10^{-3}\ \text{ps}^{-1}$) in the axial dimension and applying stress-free boundary conditions in the transverse directions. The stress−strain curve was computed using a moving average (window size = 1000 time steps) of the axial component of the instantaneous virial stress tensor:

$$\sigma_{xx} = \frac{1}{V}\left[\sum_i m_i v_{ix} v_{ix} + \sum_i r_{ix} f_{ix}\right] \quad (1)$$

where V is the volume of the simulation box, m_i is the mass of the ith particle and $\{v_{ix}, r_{ix}, f_{ix}\}$ are the axial components of the velocity, position, and force. The tensile modulus was estimated by fitting a straight line to the linear regime of the stress−strain curve, and the Poisson's ratio was calculated as $\nu = -(d\varepsilon_{trans}/d\varepsilon_{axial})$, where ε represents the engineering strain. A key assumption is that the mechanical response of the P3ATs, especially differences in mechanical properties between similar materials, is dominated by the state of the amorphous phase (i.e., glassy, leathery, fluid) at a given temperature.[33] We thus did not include the effect of partial crystallinity.[7] For each system, we repeated the procedure starting from two independent initial configurations and strained the box in all three dimensions to obtain six independent measurements of the mechanical response to uniaxial loading. Because of the extremely large size of the system, very little variation was observed between measurements. All simulations and visualization were performed using LAMMPS, VMD, and OVITO.[34−36] A complete description of the parameters used for both of the models is provided in the Supporting Information.

RESULTS AND DISCUSSION

Comparison of Models. We begin by comparing the results obtained from the one-site model and the three-site model for pure P3HT. One observation that immediately distinguishes the two models is the density that we obtained upon equilibration (snapshots of equilibrated morphologies for the two models are shown in Figure 3a). We found that the

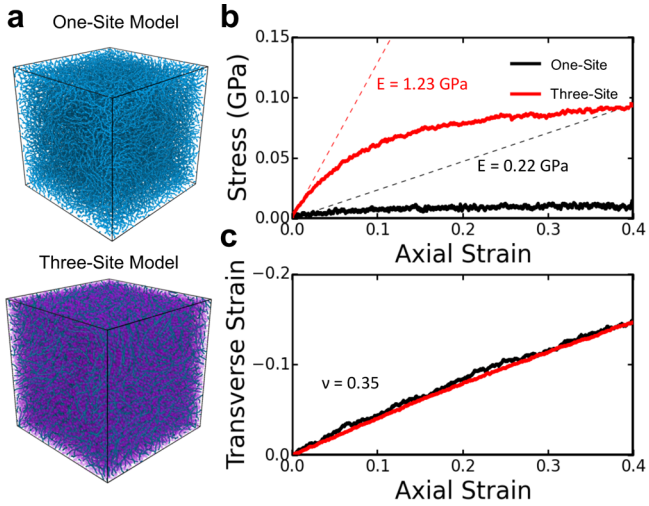

Figure 3. Simulated mechanical properties of P3HT. (a) Representative snapshots of the equilibrated morphology obtained for the one-site and three-site model. Comparison of (b) stress response and (c) transverse strain response to uniaxial loading.

three-site model equilibrated to a density of 0.955 ± 0.001 g cm^{-3} at 300 K, which is reasonable compared to the experimentally determined value of 1.094 ± 0.002 g cm^{-3} for the amorphous phase of regioregular P3HT of the same average molecular weight, measured using gas pycnometry.[37] In contrast, we obtained a value of 2.1 ± 0.07 g cm^{-3} for the one-site model, which is substantially higher than the experimental value. We attributed this discrepancy to the small value of the σ parameter (4.95 Å) in the Lennard-Jones potential for this model. It has been noted by Hsu and co-

DOI: 10.1021/acs.macromol.6b00204
Macromolecules 2016, 49, 2886−2894

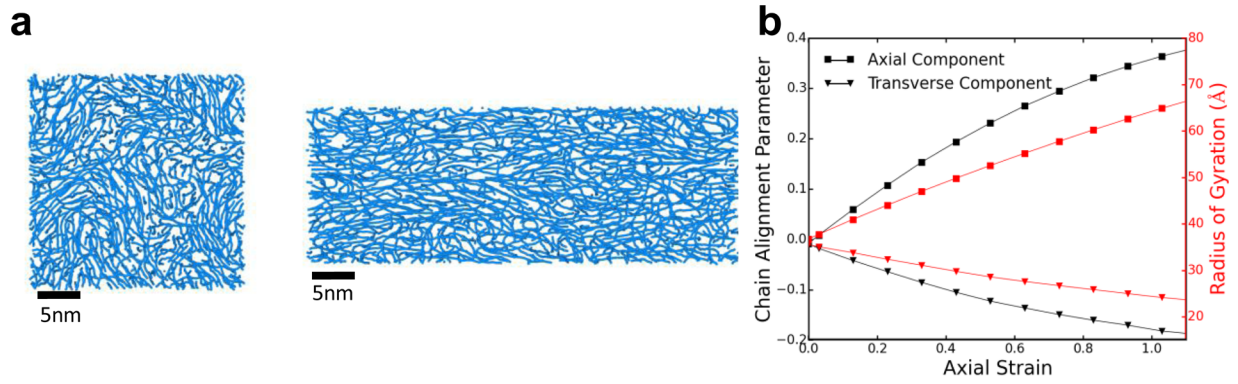

Figure 4. Simulated strain-induced chain alignment in P3HT. (a) Representative snapshots showing a thin cross section of the simulated morphology before and after straining to 100% (side chain beads not shown for clarity). (b) Plot showing the evolution of the axial and transverse components of the chain alignment parameter as well as the radius of gyration during the uniaxial loading simulation.

workers[38] that to derive thermomechanically consistent CG parameters, σ can be tuned to improve the ability of the models to reproduce the density of the target system. We found, through an iterative approach, that $\sigma \approx 8.0$ Å was required to match the density of the one-site model to that of the atomistic and three-site models. However, this modification caused the pair distribution function to depart significantly from that computed from atomistic simulations.[26] This observation highlighted the inadequacy of a one-site description of the hexylthiophene monomer and led us to the conclusion that a one-site model does not contain sufficient detail to simultaneously match the structure and the density of the underlying atomistic system.

Next, we compared the mechanical response of the two systems to uniaxial tensile loading. A representative stress–strain curve obtained from these simulations is shown in Figure 3b. We found that the three-site model predicted a tensile modulus of 1.23 ± 0.01 GPa, while the one-site model predicted a value of 0.22 ± 0.02 GPa. Comparing to the experimentally determined value of 1.09 ± 0.15 GPa, for as-cast thin films of this molecular weight, measured using the buckling method,[39] we found that the three-site model gave much closer agreement with experiment. The observation that the one-site model predicted a higher density and a lower tensile modulus indicated that not enough microscopic detail was preserved to accurately describe the microstructural packing and frictional interactions. This observation further validated our conclusion that a more detailed coarse-grained mapping is necessary to reproduce both structural and thermomechanical properties. We also found that both models predict a Poisson ratio of 0.35 (Figure 3c), which agrees with previous theoretical predictions.[40]

The results of the three-site model also compare favorably with the atomistic simulations of P3HT, which predict a value of 1.6 GPa for chain lengths of 100 monomers.[21] As might be expected, due to the inherently softer nature of the CG potentials that emerges from integrating over atomistic features, we observe that decreasing the resolution of the model leads to lower predicted values for the tensile modulus. The closer matching of the three-site model to the experimental results than the atomistic model could in part be due to the difference in the loading conditions of the two systems studied. Specifically, in the atomistic simulations, the transverse dimensions were held constant to force a Poisson ratio of zero, whereas the transverse dimensions were allowed to relax under stress-free boundary conditions in our CG simulations.

The excellent agreement observed between simulation and experiment for the three-site model motivated us to use this model further to take a closer look at morphological changes in the amorphous material induced by mechanical strain.

Strain-Induced Chain Alignment. It is well-known that applying a uniaxial strain to an amorphous or semicrystalline polymer causes the chains to plastically deform and align in the axial direction. This effect is of particular technological relevance for semiconducting polymers where the degree of chain alignment has a significant effect on the macroscopic optoelectronic properties. For example, experimental studies on P3HT have demonstrated significant anisotropy in the optical absorption and charge-transport properties for strain-aligned films, achieving an optical dichroic ratio of 4.8 and charge-mobility anisotropy of 9.[41] As shown in Figure 4a, this effect was clearly observed in our simulations.

To quantify the degree of chain alignment in the amorphous phase through the application of uniaxial strain, we computed a chain alignment order parameter.[42] The unit vector defining the orientation of each thiophene unit was calculated as the chord connecting second nearest neighbors along the backbone, $\mathbf{e}_i = (\mathbf{r}_{i+1} - \mathbf{r}_{i-1})/|\mathbf{r}_{i+1} - \mathbf{r}_{i-1}|$, and the chain alignment order parameter was computed as the second-order Legendre polynomial:

$$P_{2x} = \frac{3}{2}\langle(\mathbf{e}_i \cdot \mathbf{e}_x)^2\rangle - \frac{1}{2} \tag{2}$$

where $\mathbf{e}_x$ represents the unit vector in either the transverse or axial dimension and the angular brackets denote an average over all thiophene units. In addition, we quantified the anisotropic change in the structure of the polymer chains as the axial and transverse components of the radius of gyration tensor:

$$R_{gx} = \sqrt{\left\langle \frac{1}{M}\sum_i m_i (r_{ix} - r_{cx})^2 \right\rangle} \tag{3}$$

where M is the molecular weight of the chain, m_i is the mass of the CG bead, r_{cx} is either the axial or transverse component of the center of mass, the summation is over all i CG beads in each chain, and the angular brackets denote an average over all chains.

The evolution of axial and transverse components of P_{2x} and R_{gx} is shown in Figure 4b. Both quantities show increasing alignment of chains with increasing strain. The chain alignment

DOI: 10.1021/acs.macromol.6b00204
Macromolecules 2016, 49, 2886–2894

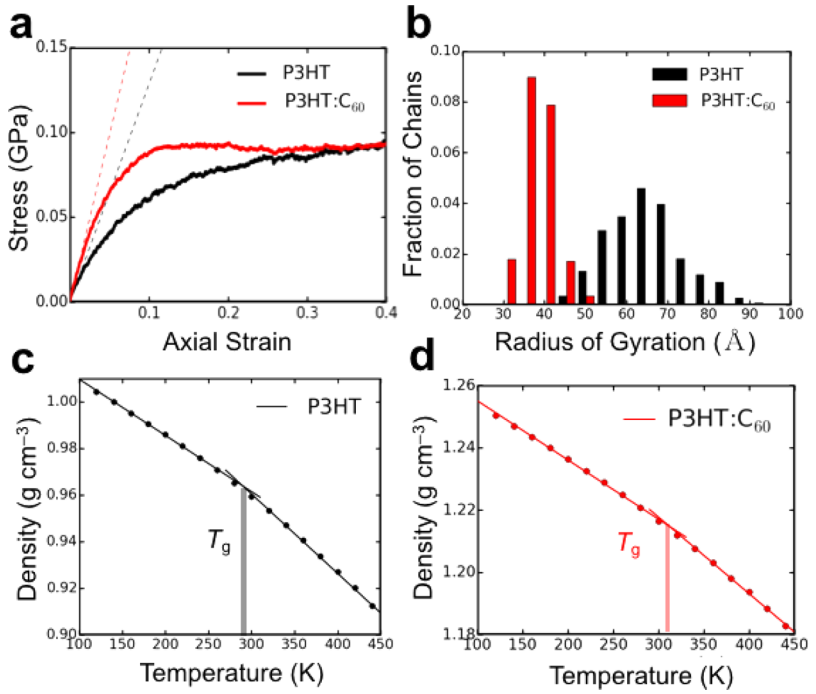

Figure 5. Comparison of predicted thermomechanical properties of pure P3HT with P3HT:C_{60}. (a) Stress−strain curve showing a transition from a melt to a glassy response with the addition of C_{60}. (b) Histogram of radius of gyration of P3HT chains in the condensed phase. Quenching curves for (c) pure P3HT and (d) P3HT:C_{60} showing an estimate for the glass transition temperature.

parameter computed here can in fact be related to the experimentally accessible optical dichroic ratio of this material: $P_{\parallel} = (R - 1)/(R + 1)$, where R is the dichroic ratio. O'Connor et al.[41] have reported a value of ∼0.36 for the chain alignment parameter of the amorphous region of a film strained to 112% using a combination of UV−vis spectroscopy and 2D grazing-incidence X-ray diffraction (assuming ∼50% crystallinity).[43] Our simulations predicted a value of 0.363 at 112% strain, which agrees remarkably well with this experimental result.

Effect of Fullerene Acceptor. One of the most important applications of semiconducting polymers is as the active material of thin-film organic photovoltaic devices. Typically, these are fabricated by solution-casting a physical blend of two semiconducting materials, an electron donor (hole-conducting) and an electron acceptor (electron-conducting), to form a phase-segregated bulk heterojunction that is bicontinuous.[44] P3HT is a commonly used electron donor material, while fullerene derivatives such as phenyl-C_{61}-butyric acid methyl ester (PCBM) are the most commonly used electron acceptors. The phase behavior of the P3HT:PCBM system is well studied, and it has been shown that this binary composite consists of three separate phases: crystalline P3HT, a PCBM-rich phase, and a mixed amorphous phase.[45] It has also been observed that the addition of PCBM to P3HT increases both the glass transition temperature[46] and the tensile modulus of the composite material (i.e., PCBM acts as an antiplasticizing agent which stiffens and embrittles the film).[47] We hypothesized that the addition of C_{60}—for which CG model parameters have been developed[23]—would have a similar effect as PCBM and tested the ability of the three-site model to predict it.

To study the effect of adding C_{60}, we applied our computational methodology to prepare a system consisting of a physical blend of P3HT with C_{60} at a 1:1 mass fraction (10 000 C_{60} molecules) using the three-site model. This system is representative of the amorphous mixed phase of the composite material (crystallization of the polymer and phase segregation do not occur over the time scales simulated). A comparison of the mechanical response to uniaxial loading is shown in Figure 5a. We observed that the addition of fullerene indeed resulted in a stiffer material, with the simulations predicting a tensile modulus of 1.92 ± 0.05 GPa. This prediction agrees well with the experimentally determined value of 1.97 ± 0.07 GPa for an as-cast thin film of P3HT:PCBM, measured using the buckling method.[48]

Interestingly, we also observed a drastic change in the distribution of the radius of gyration of the P3HT chains in the composite system. As can be seen in Figure 5b, there is an approximately 2-fold reduction in the average radius of gyration, indicating that the chains are not as well extended in the composite system. This effect is most likely due to partial phase segregation of the fullerene molecules confining the P3HT chains into a smaller volume and promoting self-interactions. We hypothesized that this reduction in the spatial extent of the polymer chains could lead to a lower density of entanglements, which may explain the significantly increased brittleness of P3HT:PCBM compared to pure P3HT that has been observed experimentally through film-on-elastomer techniques.[7] We note that no cracking or craze formation is observed in these simulations, even though experimentally the onset of cracking occurs at ∼2% strain for P3HT:PCBM.[7] To quantify this effect we applied the Z1 algorithm developed by Kröger and coworkers[49−51] to compute the primitive paths of the polymer network and compare the number of entanglements present in the two systems. We found that pure P3HT had approximately three times more entanglements than the composite system by comparing the average number of interior kinks per chain, $\langle Z \rangle$, which is proportional to entanglement density. A plot showing the primitive paths obtained for both systems, as well as the numerical values for relevant physical parameters obtained from the Z1 analysis are given in the

DOI: 10.1021/acs.macromol.6b00204
Macromolecules 2016, 49, 2886−2894

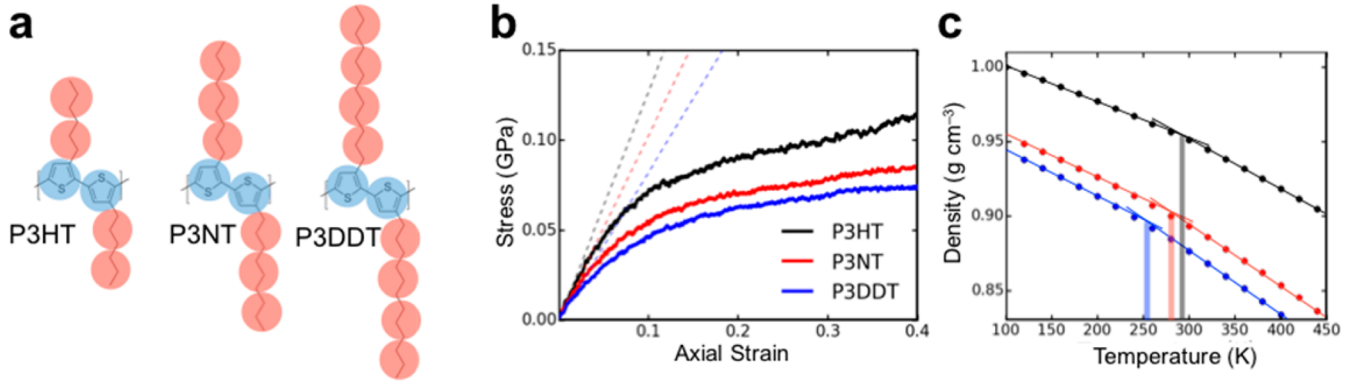

Figure 6. Predicted mechanical response of P3ATs, where A = hexyl, nonyl, and dodecyl. (a) Diagram showing the extension made to the three-site model for P3HT to allow for the simulation of P3ATs with longer alkyl side chains. (b) Stress−strain curves and (c) thermal quenching curves obtained for the three P3ATs.

Supplementary Information Figure S3 and Table S4. We attribute the absence of cracking and crazing to the fact that fracturing in polymers is usually initiated by defects at the surface, which are not present in these simulations due to periodic boundary conditions.

Thermal Properties. We next turned to predictions of the thermal properties for these systems. Of critical importance for the processing and stability of organic semiconductors is the glass transition temperature.[52] This thermal property is especially important for bulk heterojunction solar cells, which often consist of nonequilibrium structures quenched below their glass transition temperature when initially cast from solution. An important step for optimizing the photovoltaic efficiency of these devices is a postdeposition annealing step above the glass transition, which allows main-chain segmental crystallization and partial phase segregation of the bulk heterojunction components. These effects lead to a red-shifted absorption spectrum and improved extraction of photogenerated charges.[53,54] Several experimental studies using various techniques (differential scanning calorimetry,[46] dynamic mechanical thermal analysis,[55] variable temperature ellipsometry,[56] and *in situ* photovoltaic characterization[53]) have helped characterize the thermal properties of P3HT:PCBM blends. Differences in processing conditions, molecular weights, and characterization techniques have led to widely disparate experimental results. The generally agreed upon trend, however, is that the addition of PCBM acts to vitrify the P3HT.[52] Figures 5c and 5d show a comparison of the thermal quenching curves obtained for pure P3HT and P3HT:C_{60}. We predicted a value of approximately 290 and 310 K for the pure and mixed systems, respectively. Our predicted value for both systems are in excellent agreement with the experimentally determined values of 285−287 K for high-MW regioregular P3HT[52] and 313 K for 1:1 mass ratio of P3HT:PCBM.[46] The validation provided by this agreement led us to the conclusion that CG models such as these can potentially be used to understand complex structure−property relationships in semiconducting polymers, such as the effect of side-chain length.

Effect of Alkyl Side Chain Length. The basic structural motif of a semiconducting polymer is a rigid π-conjugated backbone that is functionalized with flexible aliphatic side chains. The choice of the side chain is an important criterion that plays a critical role in determining the solubility, solid-state morphology, and thermomechanical properties of the bulk material.[57] One advantage of the three-site model for P3HT is that it explicitly accounts for the hexyl side chain attached to the thiophene monomers. An important question is the transferability of this model to describe the general class of P3ATs. To extend the model, we introduced additional CG beads to the side chain, as shown in Figure 5a. Initially, we used the original parameters from the three-site model for P3HT; however, we observed trends that were in contradiction with experimental results (shown in Figure S3b), indicating that the original model was not transferable. To make the model transferrable, we adopted a similar strategy to Jankowski et al.[58] and modified the intermolecular interactions to account for the fact that the dispersive and electrostatic interactions between the CG beads representing the thiophene backbone are stronger than those between the side-chain beads. We redistributed the intermolecular cohesive energy present in the epsilon parameters of the Lennard-Jones 9−6 potential to make the potential well for the beads representing thiophene rings 3 times more attractive (7.53 kJ mol^{-1}) than the beads representing the alkyl side chains (2.51 kJ mol^{-1}) while retaining approximately the same temperature−density equations of state and elastic modulus for P3HT as shown in Figure 6b,c. We emphasize that this model is only qualitative because the modification also alters the structural distributions, and a systematic parametrization from atomistic simulations using accurate force-matching methods would be required for a quantitatively accurate and transferable model.

The predications of thermomechanical properties obtained for our modified model are shown in Figure 6b,c. We see that increasing the alkyl side chain length decreases the density, the tensile modulus, and the glass transition temperature. We predicted values of 0.99 ± 0.03 GPa for P3NT (n = 9) and 0.78 ± 0.02 GPa for P3DDT (n = 12). Although the tensile modulus of P3NT has not been measured experimentally so far, that of P3DDT has been measured to be 0.16 ± 0.07 GPa.[39] We note that the model captured the overall trend of decreasing modulus with increasing side-chain length, though the agreement with experimental results is not quantitative. The lack of transferability observed here could be due in part to the inadequacy of representing the thiophene ring as a spherical CG site; taking the anisotropic shape of the ring into account would require at least three CG sites (to form a plane). For the glass transition temperatures, we predict a value of 280 K for P3NT and 258 K for P3DDT. Comparing to the experimentally determined range of 230−258 K for P3DDT, we observe good agreement here, along with correct trends.[59,60]

DOI: 10.1021/acs.macromol.6b00204
Macromolecules 2016, 49, 2886−2894

CONCLUSION

We investigated the feasibility of using CG MD simulations to predict the thermomechanical properties of the model conjugated-polymer P3HT as well as its blend with C_{60} fullerene. Through comparisons to experimental density, elastic modulus, and glass transition temperature for the pure and composite system, we identified the optimal degree of coarse-graining required to retain the essential physics of the underlying atomistic model and achieve agreement between simulation and experiment. We then used the validated three-site model to predict the chain alignment caused by uniaxial loading and showed the effect of fullerene on the thermomechanical properties, demonstrating excellent agreement with experiment. Extension of the model to describe a range of P3ATs gave only qualitative agreement with experiment, indicating limited transferability of such models to polymers with even moderate variations in molecular structure such as the addition of three or six methylene units considered in this study. One potential approach for developing CG models with improved transferability would be to use several target atomistic systems with varied chemical structures and iteratively apply the IBI approach in such a way as to produce a set of parameters that self-consistently match all of the structural and thermodynamic data across the chosen range of chemical structures. Given the extensive validation and identification of limitations presented here, models such as these can be developed for new materials, such as the important class of donor−acceptor conjugated polymers,[61] to allow for the precise determination of structure−property relationships in organic semiconductors and aid in the molecular design of material systems exhibiting mechanical compliance for a variety of applications in mechanically robust, stretchable, and ultraflexible electronics.

ASSOCIATED CONTENT

Supporting Information

The Supporting Information is available free of charge on the ACS Publications website at DOI: 10.1021/acs.macromol.6b00204.

Complete description of model parameters used for the one-site and three-site model, results from primitive path analysis, and initial results obtained from unmodified extension to the three-site model (PDF)

AUTHOR INFORMATION

Corresponding Authors

*E-mail garya@ucsd.edu (G.A.).
*E-mail dlipomi@ucsd.edu (D.J.L.).

Notes

The authors declare no competing financial interest.

ACKNOWLEDGMENTS

This work was supported by the Air Force Office of Scientific Research (AFOSR) Young Investigator Program, Grant FA9550-12-10156, awarded to D.L. Additional support was provided by the National Science Foundation Graduate Research Fellowship under Grant DGE-114408 to S.S., the Hellman Fellowship awarded to D.L., and laboratory startup funds from the University of California, San Diego. Computational resources to support this work were provided by the Extreme Science and Engineering Discovery Environment (XSEDE) Program through the National Science Foundation Grant ACI-1053575.[62] The authors thank Prof. David Huang for sending us the files associated with his model as well as helpful discussions.

REFERENCES

(1) Kaltenbrunner, M.; White, M. S.; Głowacki, E. D.; Sekitani, T.; Someya, T.; Sariciftci, N. S.; Bauer, S. Ultrathin and Lightweight Organic Solar Cells with High Flexibility. *Nat. Commun.* **2012**, *3*, 770.

(2) Lipomi, D. J.; Tee, B. C.-K.; Vosgueritchian, M.; Bao, Z. Stretchable Organic Solar Cells. *Adv. Mater.* **2011**, *23*, 1771−1775.

(3) Facchetti, A. π-Conjugated Polymers for Organic Electronics and Photovoltaic Cell Applications †. *Chem. Mater.* **2011**, *23*, 733−758.

(4) Sokolov, A. N.; Atahan-Evrenk, S.; Mondal, R.; Akkerman, H. B.; Sánchez-Carrera, R. S.; Granados-Focil, S.; Schrier, J.; Mannsfeld, S. C. B.; Zoombelt, A. P.; Bao, Z.; et al. From Computational Discovery to Experimental Characterization of a High Hole Mobility Organic Crystal. *Nat. Commun.* **2011**, *2*, 437.

(5) Brédas, J. L.; Beljonne, D.; Coropceanu, V.; Cornil, J. Charge-Transfer and Energy-Transfer Processes in π-Conjugated Oligomers and Polymers: A Molecular Picture. *Chem. Rev.* **2004**, *104*, 4971−5003.

(6) Jackson, N. E.; Savoie, B. M.; Chen, L. X.; Ratner, M. A. A Simple Index for Characterizing Charge Transport in Molecular Materials. *J. Phys. Chem. Lett.* **2015**, *6*, 1018−1021.

(7) Savagatrup, S.; Printz, A. D.; O'Connor, T. F.; Zaretski, A. V.; Rodriquez, D.; Sawyer, E. J.; Rajan, K. M.; Acosta, R. I.; Root, S. E.; Lipomi, D. J. Mechanical Degradation and Stability of Organic Solar Cells: Molecular and Microstructural Determinants. *Energy Environ. Sci.* **2015**, *8*, 55−80.

(8) Yang, F.; Ghosh, S.; Lee, L. J. Molecular Dynamics Simulation Based Size and Rate Dependent Constitutive Model of Polystyrene Thin Films. *Comput. Mech.* **2012**, *50*, 169−184.

(9) Lee, S.; Rutledge, G. C. Plastic Deformation of Semicrystalline Polyethylene by Molecular Simulation. *Macromolecules* **2011**, *44*, 3096−3108.

(10) Capaldi, F. M.; Boyce, M. C.; Rutledge, G. C. Molecular Response of a Glassy Polymer to Active Deformation. *Polymer* **2004**, *45*, 1391−1399.

(11) Kim, J. M.; Locker, R.; Rutledge, G. C. Plastic Deformation of Semicrystalline Polyethylene under Extension, Compression, and Shear Using Molecular Dynamics Simulation. *Macromolecules* **2014**, *47*, 2515−2528.

(12) Agrawal, V.; Arya, G.; Oswald, J. Simultaneous Iterative Boltzmann Inversion for Coarse-Graining of Polyurea. *Macromolecules* **2014**, *47*, 3378−3389.

(13) Peter, C.; Kremer, K. Multiscale Simulation of Soft Matter Systems − from the Atomistic to the Coarse-Grained Level and Back. *Soft Matter* **2009**, *5*, 4357−4366.

(14) Kremer, K.; Grest, G. S. Dynamics of Entangled Linear Polymer Melts: A Molecular - Dynamics Simulation. *J. Chem. Phys.* **1990**, *92*, 5057−5086.

(15) Arman, B.; Reddy, A. S.; Arya, G. Viscoelastic Properties and Shock Response of Coarse-Grained Models of Multiblock versus Diblock Copolymers: Insights into Dissipative Properties of Polyurea. *Macromolecules* **2012**, *45*, 3247−3255.

(16) Reith, D.; Pütz, M.; Müller-Plathe, F. Deriving Effective Mesoscale Potentials from Atomistic Simulations. *J. Comput. Chem.* **2003**, *24*, 1624−1636.

(17) Dang, M. T.; Hirsch, L.; Wantz, G. P3HT:PCBM, Best Seller in Polymer Photovoltaic Research. *Adv. Mater.* **2011**, *23*, 3597−3602.

(18) Marcon, V.; Raos, G. Free Energies of Molecular Crystal Surfaces by Computer Simulation: Application to Tetrathiophene. *J. Am. Chem. Soc.* **2006**, *128*, 1408−1409.

(19) Dubay, K. H.; Hall, M. L.; Hughes, T. F.; Wu, C.; Reichman, D. R.; Friesner, R. A. Accurate Force Field Development for Modeling Conjugated Polymers. *J. Chem. Theory Comput.* **2012**, *8*, 4556−4569.

DOI: 10.1021/acs.macromol.6b00204
Macromolecules 2016, 49, 2886−2894

(20) Jackson, N. E.; Kohlstedt, K. L.; Savoie, B. M.; Olvera de la Cruz, M.; Schatz, G. C.; Chen, L. X.; Ratner, M. A. Conformational Order in Aggregates of Conjugated Polymers. *J. Am. Chem. Soc.* **2015**, *137*, 6254−6262.
(21) Tummala, N. R.; Risko, C.; Bruner, C.; Dauskardt, R. H.; Brédas, J.-L. Entanglements in P3HT and Their Influence on Thin-Film Mechanical Properties: Insights from Molecular Dynamics Simulations. *J. Polym. Sci., Part B: Polym. Phys.* **2015**, *53*, 1−9.
(22) Tummala, N. R.; Bruner, C.; Risko, C.; Brédas, J.-L.; Dauskardt, R. H. Molecular-Scale Understanding of Cohesion and Fracture in P3HT:Fullerene Blends. *ACS Appl. Mater. Interfaces* **2015**, *7*, 9957−9964.
(23) Huang, D. M.; Faller, R.; Do, K.; Moule, A. J. Coarse-Grained Computer Simulations of Polymer/Fullerene Bulk Heterojunctions for Organic Photovoltaic Applications. *J. Chem. Theory Comput.* **2010**, *6*, 526−537.
(24) Schwarz, K. N.; Kee, T. W.; Huang, D. M. Coarse-Grained Simulations of the Solution-Phase Self-Assembly of poly(3-Hexylthiophene) Nanostructures. *Nanoscale* **2013**, *5*, 2017−2027.
(25) To, T. T.; Adams, S. Modelling of P3HT:PCBM Interface Using Coarse-Grained Forcefield Derived from Accurate Atomistic Forcefield. *Phys. Chem. Chem. Phys.* **2014**, *16*, 4653−4663.
(26) Lee, C.-K.; Pao, C.-W.; Chu, C.-W. Multiscale Molecular Simulations of the Nanoscale Morphologies of P3HT:PCBM Blends for Bulk Heterojunction Organic Photovoltaic Cells. *Energy Environ. Sci.* **2011**, *4*, 4124−4132.
(27) Lee, C. K.; Pao, C. W. Nanomorphology Evolution of p3ht/pcbm Blends during Solution-Processing from Coarse-Grained Molecular Simulations. *J. Phys. Chem. C* **2014**, *118*, 11224−11233.
(28) Do, K.; Risko, C.; Anthony, J. E.; Amassian, A.; Bredas, J.-L. Dynamics, Miscibility, and Morphology in Polymer-Molecule Blends: The Impact of Chemical Functionality. *Chem. Mater.* **2015**, *27*, 7643−7651.
(29) Chen, C.-W.; Huang, C.-I. Effects of Intra/inter-Molecular Potential Parameters, Length and Grafting Density of Side-Chains on the Self-Assembling Behavior of poly(3′-Alkylthiophene)s in the Ordered State. *Polymer* **2015**, *77*, 189−198.
(30) Jones, M. L.; Huang, D. M.; Chakrabarti, B.; Groves, C. Relating Molecular Morphology to Charge Mobility in Semicrystalline Conjugated Polymers. *J. Phys. Chem. C* **2016**, *120*, 4240−4250.
(31) Karayiannis, N. C.; Kröger, M. Combined Molecular Algorithms for the Generation, Equilibration and Topological Analysis of Entangled Polymers: Methodology and Performance. *Int. J. Mol. Sci.* **2009**, *10*, 5054−5089.
(32) Allen, M. P.; Tildesley, D. J. *Computer Simulation of Liquids*; Oxford University Press: Clarendon, Oxford, 1987.
(33) Savagatrup, S.; Printz, A. D.; Wu, H.; Rajan, K. M.; Sawyer, E. J.; Zaretski, A. V.; Bettinger, C. J.; Lipomi, D. J. Viability of Stretchable poly(3-Heptylthiophene) (P3HpT) for Organic Solar Cells and Field-Effect Transistors. *Synth. Met.* **2015**, *203*, 208−214.
(34) Plimpton, S. Fast Parallel Algorithms for Short-Range Molecular Dynamics. *J. Comput. Phys.* **1995**, *117*, 1−19.
(35) Humphrey, W.; Dalke, A.; Schulten, K. VMD: Visual Molecular Dynamics. *J. Mol. Graphics* **1996**, *14*, 33−38.
(36) Stukowski, A. Visualization and Analysis of Atomistic Simulation Data with OVITO−the Open Visualization Tool. *Modell. Simul. Mater. Sci. Eng.* **2010**, *18*, 015012.
(37) Lee, C. S.; Dadmun, M. D. Important Thermodynamic Characteristics of poly(3-Hexyl Thiophene). *Polymer* **2014**, *55*, 4−7.
(38) Hsu, D. D.; Xia, W.; Arturo, S. G.; Keten, S. Systematic Method for Thermomechanically Consistent Coarse-Graining: A Universal Model for Methacrylate-Based Polymers. *J. Chem. Theory Comput.* **2014**, *10*, 2514−2527.
(39) Savagatrup, S.; Makaram, A. S.; Burke, D. J.; Lipomi, D. J. Mechanical Properties of Conjugated Polymers and Polymer-Fullerene Composites as a Function of Molecular Structure. *Adv. Funct. Mater.* **2014**, *24*, 1169−1181.
(40) Tahk, D.; Lee, H. H.; Khang, D.-Y. Elastic Moduli of Organic Electronic Materials by the Buckling Method. *Macromolecules* **2009**, *42*, 7079−7083.
(41) O'Connor, B.; Kline, R. J.; Conrad, B. R.; Richter, L. J.; Gundlach, D.; Toney, M. F.; DeLongchamp, D. M. Anisotropic Structure and Charge Transport in Highly Strain-Aligned Regioregular poly(3-Hexylthiophene). *Adv. Funct. Mater.* **2011**, *21*, 3697−3705.
(42) Lavine, M. S.; Waheed, N.; Rutledge, G. C. Molecular Dynamics Simulation of Orientation and Crystallization of Polyethylene during Uniaxial Extension. *Polymer* **2003**, *44*, 1771−1779.
(43) Zen, A.; Saphiannikova, M.; Neher, D.; Grenzer, J.; Grigorian, S.; Pietsch, U.; Asawapirom, U.; Janietz, S.; Scherf, U.; Lieberwirth, I.; et al. Effect of Molecular Weight on the Structure and Crystallinity of poly(3-Hexylthiophene). *Macromolecules* **2006**, *39*, 2162−2171.
(44) Scharber, M. C.; Muehlbacher, D.; Koppe, M.; Denk, P.; Waldauf, C.; Heeger, A. J.; Brabec, C. J. Design Rules for Donors in Bulk Heterojunction Solar Cells Towards 10% Energy Conversion Efficiency. *Adv. Mater.* **2006**, *18*, 789−794.
(45) Treat, N. D.; Chabinyc, M. L. Phase Separation in Bulk Heterojunctions of Semiconducting Polymers and Fullerenes for Photovoltaics. *Annu. Rev. Phys. Chem.* **2014**, *65*, 59−81.
(46) Zhao, J.; Swinnen, A.; Van Assche, G.; Manca, J.; Vanderzande, D.; Van Mele, B. Phase Diagram of P3HT/PCBM Blends and Its Implication for the Stability of Morphology. *J. Phys. Chem. B* **2009**, *113*, 1587−1591.
(47) Savagatrup, S.; Printz, A. D.; Rodriquez, D.; Lipomi, D. J. Best of Both Worlds: Conjugated Polymers Exhibiting Good Photovoltaic Behavior and High Tensile Elasticity. *Macromolecules* **2014**, *47*, 1981−1992.
(48) Printz, A. D.; Savagatrup, S.; Rodriquez, D.; Lipomi, D. J. Role of Molecular Mixing on the Stiffness of Polymer:fullerene Bulk Heterojunction Films. *Sol. Energy Mater. Sol. Cells* **2015**, *134*, 64−72.
(49) Kröger, M. Shortest Multiple Disconnected Path for the Analysis of Entanglements in Two- and Three-Dimensional Polymeric Systems. *Comput. Phys. Commun.* **2005**, *168*, 209−232.
(50) Hoy, R. S.; Foteinopoulou, K.; Kröger, M. Topological Analysis of Polymeric Melts: Chain-Length Effects and Fast-Converging Estimators for Entanglement Length. *Phys. Rev. E - Stat. Nonlinear, Soft Matter Phys.* **2009**, *80*, 14−16.
(51) Shanbhag, S.; Kröger, M. Primitive Path Networks Generated by Annealing and Geometrical Methods: Insights into Differences. *Macromolecules* **2007**, *40*, 2897−2903.
(52) Müller, C. On the Glass Transition of Polymer Semiconductors and Its Impact on Polymer Solar Cell Stability. *Chem. Mater.* **2015**, *27*, 2740−2754.
(53) Treat, N. D.; Shuttle, C. G.; Toney, M. F.; Hawker, C. J.; Chabinyc, M. L. In Situ Measurement of Power Conversion Efficiency and Molecular Ordering during Thermal Annealing in P3HT:PCBM Bulk Heterojunction Solar Cells. *J. Mater. Chem.* **2011**, *21*, 15224−15231.
(54) Li, G.; Shrotriya, V.; Huang, J.; Yao, Y.; Moriarty, T.; Emery, K.; Yang, Y. High-Efficiency Solution Processable Polymer Photovoltaic Cells by Self-Organization of Polymer Blends. *Nat. Mater.* **2005**, *4*, 864−868.
(55) Hopkinson, P. E.; Staniec, P. A.; Pearson, A. J.; Dunbar, A. D. F.; Wang, T.; Ryan, A. J.; Jones, R. A. L.; Lidzey, D. G.; Donald, A. M. A Phase Diagram of the P3HT:PCBM Organic Photovoltaic System: Implications for Device Processing and Performance. *Macromolecules* **2011**, *44*, 2908−2917.
(56) Pearson, A. J.; Wang, T.; Jones, R. a L.; Lidzey, D. G.; Staniec, P. A.; Hopkinson, P. E.; Donald, A. M. Rationalizing Phase Transitions with Thermal Annealing Temperatures for P3HT:PCBM Organic Photovoltaic Devices. *Macromolecules* **2012**, *45*, 1499−1508.
(57) Mei, J.; Bao, Z. Side Chain Engineering in Solution-Processable Conjugated Polymers. *Chem. Mater.* **2014**, *26*, 604−615.
(58) Jankowski, E.; Marsh, H. S.; Jayaraman, A. Computationally Linking Molecular Features of Conjugated Polymers and Fullerene Derivatives to Bulk Heterojunction Morphology. *Macromolecules* **2013**, *46*, 5775−5785.

DOI: 10.1021/acs.macromol.6b00204
Macromolecules 2016, 49, 2886−2894

(59) Pankaj, S.; Hempel, E.; Beiner, M. Side-Chain Dynamics and Crystallization in a Series of Regiorandom Poly(3-Alkylthiophenes). *Macromolecules* **2009**, *42*, 716−724.
(60) Pankaj, S.; Beiner, M. Confined Dynamics and Crystallization in Self-Assembled Alkyl Nanodomains. *J. Phys. Chem. B* **2010**, *114*, 15459−15465.
(61) Sirringhaus, H. 25th Anniversary Article: Organic Field-Effect Transistors: The Path Beyond Amorphous Silicon. *Adv. Mater.* **2014**, *26*, 1319−1335.
(62) John, T.; Cockerill, T.; Foster, I.; Gaither, K. XSEDE: Accelerating Scientific Discovery. *Comput. Sci. Eng.* **2014**, *16*, 62−74.

DOI: 10.1021/acs.macromol.6b00204
Macromolecules 2016, 49, 2886−2894